의학박사 학위논문

전립선암 세포주에서 vascular disrupting agent 인 CKD-516 의 항암 효과와 기전 연구

Anticancer Effects and Mechanisms of Vascular Disrupting Agent, CKD-516, in Prostate Cancer Cell Lines

울산대학교 대학원

의 학 과

이 원 철

Anticancer Effects and Mechanisms of Vascular Disrupting Agent, CKD-516, in Prostate Cancer Cell Lines

지 도 교 수　　김 청 수

이 논문을 의학박사 학위 논문으로 제출함

2021 년 2 월

울 산 대 학 교 대 학 원

의　학　과

이 원 철

이원철의 의학박사학위 논문을 인준함

심사위원 홍 준 혁 (인)

심사위원 김 청 수 (인)

심사위원 홍 범 식 (인)

심사위원 김 건 석 (인)

심사위원 한 준 현 (인)

울 산 대 학 교 대 학 원

2021 년 2 월

ABSTRACT

Purpose: CKD-516 is a novel vascular disrupting agent. In this study, we investigated the anticancer effects and mechanisms of CKD-516 on prostate cancer cell line and animal model. Furthermore, we investigated the synergistic effect of combination therapy with CKD-516 and immune checkpoint inhibitor.

Material and methods: S-516, the active metabolite of CKD-516, was used for in vitro studies. The mouse prostate epithelial adenocarcinoma cell line TRAMP-C1 and human prostate cancer cell lines including PC3, DU145, LNCaP, and 22Rv1 were obtained. Cell viability assay was performed and mechanisms of CKD-516 was confirmed by western blot analysis. For in vivo analysis, TRAMP-C1 cells were implanted into the mice and CKD-516 was administered via oral gavage at 3mg/kg or 6mg/kg twice per week for 3 weeks. For combination therapy studies, anti-PD-1 was injected 5mg/kg twice per week for 3 weeks. Dendritic cell(DC) was obtained to verify maturation effect of CKD-516 on DC.

Results: S-516 inhibited the cell viability of all prostate cancer cells in a concentration-dependent manner, with IC_{50} values of of 0.045 μmol/L, DU145 and LNCaP-0.04 μmol/L, 22Rv-0.004 μmol/L and TRAMP-C1 0.68 μmol/L. S-516 induced apoptosis of prostate cancer cell lines by phosphorylation of c-JUN and JNK. In vivo studies demonstrated significant synergistic effect by using both CKD-516 and anti-PD-1. The percentage of

tumor growth inhibition was significantly higher in the combination therapy group.(34.64% in CKD-516 3mg/kg, 90.69% in CKD-516 and anti-PD-1 combination therapy). DC maturation was induced by CKD-516 and expression of cell surface markers such as CD80 and CD86 were significantly increased.

Conclusions: CKD-516 is a promising agent inducing apoptosis of tumor cells and enhances anticancer effect in combination with an immune checkpoint inhibitor.

Key words; Prostate cancer cell lines, CKD-516, Vascular disrupting agent, Anti-PD-1

CONTENTS

List of Tables

List of Figures

List of Abbreviations

BSA; Bovine serum albumin

CRPC; Castration-resistant prostate cancer

DNA; Deoxyribonucleic acid

FBS; Fetal bovine serum

GAPDH; Glyceraldehyde 3-phosphoate dehydrogenase

LPS; Lipopolysaccharide

MoDC; Monocyte-Derived dendritic cell

PAGE; Polyacrylamide gel electrophoresis

PARP; Poly(ADP-ribose)polymerase

PBS; Phosphate-buffered saline

PI; Propidium iodide

PVDF; Polyvinyl fluoride

VDA; Vascular disrupting agent

Introduction

Prostate cancer is the second most common malignancy in men which accounts about 3.8% of all deaths caused by cancer in men.[1] Although most newly detected prostate cancers are androgen dependent which could be cured by androgen deprivation therapy(ADT), the tumor adaptation to ADT leads to the formation of castration-resistant prostate cancer(CRPC) which is frequently metastatic and lethal.[2] Progression to the castration-resistant state is associated with changes in vascular morphology and increased angiogenesis.[3]

Throughout the past decades, tumor neo-vasculature was a significant target in cancer treatment due to the dependence of tumor growth on vascular network.[4] Compared to the normal vasculature, the tumor vasculature has an incomplete, naive structure.[5] Vascular disrupting agents(VDAs) selectively breakdown established tumor vasculature and induce cancer cell death in the tumor core.[6] VDAs act by breaking the endothelium of solid tumors resulting in the tumor death from the lack of oxygen and mineral leading to tumor cell ischemia and necrosis. VDAs differ from the conventional angiogenesis inhibitor as the latter prohibits the formation of new blood vessels while VDAs selectively target pre-existing tumor vasculature. There are two main types of VDAs. One is ligand-dependent agents and the other is small-molecule anti-vascular agents.[7]

Microtubules are long, filamentous, tubular shaped protein polymers that play a significant role in the development and maintenance of cell shape. They are composed of α-β tubulin heterodimers that arrange the cytoplasm during interphase. Their role is to separate condensed chromosomes during mitosis. Anti-mitotic agents that interfere with the microtubule assembly are key components of combination chemotherapies for the treatment of various cancers.[8]

CKD-516(Valecobulin), a novel small-molecule VDA which prohibits microtubule polymerization, was developed recently. CKD-516 is a valine prodrug of S-516 and is a benzophenone analog with a modification of the B ring, which is replaced by a carbonyl group.[9] S-516 was modified to CKD-516 to increase water solubility and expected to be released from CKD-516 in vivo by various peptidases. S-516 demonstrates potent cytotoxicity against several cancer cells including the P-gp overexpressing mutltidrug-resistant(MDR) positive human xenograft HCT15 cell line.[4] In vitro studies have shown that S-516 had more cytotoxicity than other VDAs such as CA-4P and AC7700, and this was further proved in tubulin binding assay and cell cycle arrest. Moreover, CKD-516 has shown marked antitumor effect in various human tumor xenograft models, which is superior to CA-4P and AC7700. Positron emission tomography imaging showed that CKD-516 inhibited the uptake of [18F]-fluorodeoxyglucose into tumor tissue in mouse and lasted 48h after a single administration indicating VDA activity.[9]

During the last decade, several agents have been FDA-approved for the treatment of metastatic CRPC resulting in significant improvements in overall survival (OS).[10-15] However, the clinical benefit with each individual agent is rarely durable and the median OS in the castrate-resistant phase of the disease is only approximately 2–3 years.[16]

Recently, the KENOTE-028 and -199 studies demonstrated that in small portion of metastatic CRPC patients, PD-1 inhibitors were very durable and efficient but majority of the patients enrolled in this study did not benefit from the use of PD-1 inhibitor monotherapy after proper chemotherapy.[16] For this reason, there was always a great demand for the development of novel agents and combined treatments of these agents to conventional treatment modality to increase survival outcomes were proposed.

Therefore, in this study, we evaluated the therapeutic effect of a novel antitumor agent CKD-516 on human prostate cancer cells using xenograft mouse model. Furthermore, the efficacy of combination therapy with CDK-516 and PD-1 inhibitor were compared with single use of CKD-516.

MATERIALS AND METHODS

Reagents and antibodies

CKD-516 and S-516 were obtained from Chong Kun Dang Pharmaceutical Corporation (Seoul, Korea). Anti-mouse PD-1 was purchased from BioXCell (NH, USA). CKD-516 was dissolved in purified water and anti-PD-1 antibody was dissolved in normal saline for animal experiments. S-516 was dissolved in dimethylsulfoxide. The following primary antibodies were used: phospho-JNK1(threonine 183)/2(threonine 183)/3(threonine 221), JNK1/2/3, phospho c-JUN (serine 73), c-JUN, caspase-3, cleaved caspase-3, caspase-9, poly (ADP-ribose) polymerase (PARP)-1, CD80, CD86, α-tubulin, phospho-H3 (serine 10), phospho-cdc2 (threonine 15), thymidine kinase 1, cyclin B1, GAPDH and β-actin. Antibodies used in this study were summarized in Table 1.

Table 1. Primary antibodies used in this study

Antibody	Cat. No.	Dilution factor	Species	Size (molecular weight, kDa)	Manufacture	Application
phospho-JNK1/2/3 (phospho T183/T183/T183)	ab124956	1:1,000	Rabbit	46/54	abcam	WB
JNK1/2/3	ab179461	1:1,000	Rabbit	46/54	abcam	WB
phospho-c-JUN	3270	1:1,000	Rabbit	48	Cell Signaling Technology	WB
c-JUN	9165	1:1,000	Rabbit	48	Cell Signaling Technology	WB
β-actin	Sc-47778	1:10,000	Mouse	43	Santa Cruz Biotechnology	WB
PARP	9542	1:1,000	Rabbit	89/116	Cell Signaling Technology	WB
Caspase-3	9662	1:1,000	Rabbit	17/19/35	Cell Signaling Technology	WB
Cleaved caspase-3	9664	1:1,000	Rabbit	17/19	Cell Signaling Technology	WB, IHC
Caspase-9	ab202068	1:1,000	Rabbit	46	abcam	WB
GAPDH	sc-365062	1:10,000	Mouse	37	Santa Cruz Biotechnology	WB
CD80 monoclonal antibody, FITC	11-0801-81		Rat		Invitrogen	Flow Cyt
CD86 monoclonal antibody, APC	17-0862-81		Rat		Invitrogen	Flow Cyt
Thymidine Kinase1	28755	1:1,000	Rabbit	26	Cell Signaling Technology	WB
phospho-Histone H3 (Ser3)	53348	1:1,000	Rabbit	17	Cell Signaling Technology	WB
Cyclin B1	12231	1:1,000	Rabbit	55	Cell Signaling Technology	WB

phospho-cdc2 (Tyr15)	4539	1:1,000	Rabbit	34	Cell Signaling Technology	WB
α-Tubulin	2125	1:500	Rabbit	52	Cell Signaling Technology	IF

WB; western blot, IF; immune fluorescence, IHC; immunohistochemistry, Flow Cyt; flow cytometry

Cell culture

The mouse prostate epithelial adenocarcinoma cell line TRAMP-C1, as well as the human prostate cancer cell lines PC3, DU145, LNCaP and 22Rv1, were obtained from the American Type Culture Collection (ATCC). Human prostate cancer cell lines were maintained in RPMI 1640 medium with 5–10% of heat-inactivated fetal bovine serum (FBS), 1% antibiotics-antimycotics, whereas TRAMP-C1 cell lines were maintained in DMEM medium supplemented with 0.005 mg/ml bovine insulin and 10nM dehydroisoandrosterone, 1% antibiotics-antimycotics, 5% of FBS, 5% of Nu-Serum IV. All cells were cultured in 5% CO_2 atmosphere at 37 °C incubator. Cell passages from 8 to less than 20 were used in the experiments.

Cell viability assay

Cells were seeded in 96-well plates (2-3 x 10^3 cells) and exposed with 0 to 50 μmol/L S-516 for 72 hours. Cell viability assay was determined by Celltiter Glo® luminescent assay (Promega; Madison, WI, USA). After treatment with S-516, 20μL CellTiter-Glo reagents were added. The plate was incubated for 10 minutes, and then signals were measured on a VICTOR X3 luminometer (PerkinElmer;MC, USA). All plates had blank wells containing

cell-free medium to obtain a value for background luminescence. Data represented the percentage of untreated cells [(treatment value - blank) ÷ (vehicle value - blank)] expressed as the mean ± standard deviation (SD) of at least three replications. Results were analyzed using GraphPad Prism® version 8.00 (GraphPad Software; San Diego, CA, USA). In addition, the half maximal inhibitory concentration (IC_{50}) for each drug for each cell line was presented in Table 2.

Table 2. Summary of IC_{50} values and percentage cell viability of S-516 treated cancer cell lines as obtained from Celltiter Glo® luminescent assay after 72 hours of exposure.

Tissue Sources	Cell lines	IC_{50} for S-516 (µM)
Human	PC3	4.769 (0.911 to 75.65)
Human	DU145	0.045 (0.326 to 69.81)
Human	LNCaP	0.041 (0.0137 to 0.123)
Human	22Rv1	0.004 (0.0006 to 0.03)
Mouse	TRAMP-C1	0.684 (0.084 to 5.574)

Western blot analysis of whole cell lysates

Whole cell lysates were prepared in a RIPA lysis buffer containing protease inhibitor cocktails (Sigma Aldrich; St. Louis, MO, USA). The cell lysates were micro-centrifuged at 13,000 ×*g* for 5 min, and the supernatants were stored at 4 °C. Then, the protein concentration was measured using the Bradford protein assay (Bio-rad;Hercules, CA, USA). Equal amounts of proteins (10-20 μg in 15-20 μL) were subjected to sodium dodecyl sulfate (SDS)-polyacrylamide gel electrophoresis (PAGE), and electrophoretically transferred to a polyvinylidene fluoride (PVDF, company) membrane. After blocking with 5% bovine serum albumin (BSA) for 1 hour at room temperature (RT), the membranes were incubated with primary antibodies overnight at 4 °C with shaking (100 rpm). Then, the membranes were incubated with peroxidase-conjugated secondary antibodies for 1hour at RT. Immuno-reactive bands were visualized on X-ray film (Fujiflim; Tokyo, Japan) using Immunobilion Western enhanced chemiluminescent (ECL) solution (Millipore corp; Bedford, MA, USA). Membranes were stripped and re-probed with Glyceraldehyde 3-phosphate dehydrogenase (GAPDH) and β-actin antibodies to confirm equal protein loading.

Tumor injections, evaluations and drug treatment

All procedures have been reviewed and approved by the Institutional Animal Care and Use Committee (IACUC) of Asan Medical Center (# 2019-12-229). TRAMP-C1 cells used for *in vivo* studies were passaged 3 times prior to injection into mice. Cells were harvested during exponential growth and resuspended in a 1:1 mixture of PBS and Matrigel (BD Bioscience). Cells at a density of 5 x 10^6 cells/mouse were subcutaneously (s.c) injected into the right flank region of 6 weeks old male C57BL/6 mice (Central Lab. Inc., Seoul, Korea). After one week when the tumor volume was approximately 50-70 mm^3, the mice were randomly divided into control and treatment groups. For combination therapy studies, CKD-516 was administered via oral gavage at 3 mg/kg or 6 mg/kg twice per week and anti-PD-1 was administered i.p 5mg/kg twice per week for 3 weeks. The tumor measurements were evaluated using calipers; tumor volumes (mm^3) were monitored three times per 1 week and calculated using the following formula length x $width^2$ x 0.5 (length is the longest diameter and width is the shortest diameter perpendicular to length). At the end of the examination period, the tumor was extracted and weighed. The tumors then underwent protein extraction and western blot was performed.

Bone marrow-derived DC culture

Bone marrow-derived DCs (BMDCs) were induced from bone marrow (BM) cells obtained from specific pathogen-free female C57BL/6 mice, 5 weeks old (OrientBio Co., Sungnam, Korea). Mononuclear cells from BM were obtained from tibia and femur of C57BL/6 mouse sacrificed by cervical dislocation. Cells were isolated from the BM cells by MACS lineage cell depletion kit (Miltenyi Biotec; Bergisch Gladbach, Germany) and cultured with GM-CSF and IL-4 (1 x 10^3 units/ml each) at 37℃ for 4 days in a humidified CO_2 incubator for monocyte-derived dendritic cells differentiation. At day 2, fresh medium with GM-CSF and IL-4 was added to each dish. Only unadherent cells (DCs) were harvested and seeded in a fresh dish; 2 ml fresh medium including GM-CSF and IL-4 was added at day 4. Cells were also treated with S-516 (50, 100, 200 nM) and lipopolysaccharide (LPS; Sigma, 50 μg/ml) for 24 hours. S-516 or LPS-treated DCs were collected and performed western-blot and flow cytometry.

Flow cytometry analysis of DC phenotypes

The S-516 or LPS-treated DCs were collected after days 5, washed with PBS, and divided into several fractions of 5 x 10^5 cells/100 μl. Each sample was measured in triplicate. FITC-labeled anti-CD80 and APC-labeled CD86 were added into the suspension to a final

concentration of 2.5 μg/ml and incubated for 30 min at 4℃ in the dark. The cells were washed with PBS and analyzed by flow cytometry. Fluorescence-labeled IgG isotypes were used as the control.

Annexin V staining apoptosis assay

Cells were seeded in 6-well plates (3.5-5 X 10^5 cells/well) containing 10% of FBS for 18–24 h. After incubation with S-516 for 72 hours, apoptotic and necrotic cell death was assessed via flow cytometry using the annexin V-FITC apoptosis detection kit (BD Biosciences; Bedford, MA, USA), according to the manufacturer's instructions. In this assay, cells positive for annexin V and those positive for both annexin V and propidium iodide (PI) represent the early and late apoptotic populations, respectively, whereas cells positive for PI only represent the necrotic population.

Cell cycle distribution analysis

Cells were seeded in 6-well plates (3.5-5 X 10^5 cells/well) containing 10% of FBS for 18–24 h. After incubation with S-516 for 24 hours, cells were collected, washed with phosphate buffered saline (PBS) and fixed in 70% ethanol at -20 °C for at least 30 min. Then

cells were washed PBS, stained with propidium iodide (PI) solution (0.05% Triton X-100, 100 μg/ml RNAse A (Sigma aldrich)) for 30 min. Deoxyribonucleic acid(DNA) contents were analyzed by flow cytometry using FACS Calibur (BD Bioscences).

Immunofluorescence

To confirm the tubulin polymerization, cells were seeded in round slide glass, pre-coated with poly-L-lysine of a 12 well plate (6-8 x 10^4 cells/well) containing FBS. And then cells were treated with S-516 for 24 hours. Cells were fixed with 4% paraformaldehyde in PBS for 20 minutes, permeabilized with 0.1% Triton X-100 in PBS for 30 minutes. After blocking with 5% BSA in PBS for 1 hour, cells were incubated overnight at 4°C with primary antibodies against α-tubulin (1:1,000) followed by Alexa Fluor 555-labeled secondary antibody (Molecular Probes, Waltham, MA, USA) (1: 600) for 1 hour in the dark at room temperature for 1 hour. After rinsing three times in PBS, the coverslips were mounted in Vectashield with DAPI mounting medium (Vector Laboratories, Burlingame, CA, USA) for 10 minutes then sealed with nail oil. Alexa-555 and DAPI were detected and captured images with fluorescence inverted microscope (Axio Observer.Z1, Carl Zeiss Co. Ltd., Oberkochen, Germany).

Statistical analysis

Data represent the means ± SD of at least three independent experiments. Statistical analysis of the results was performed using one-way analysis of variance (ANOVA). A p-value < 0.05 was considered statistically significant.

RESULTS

The effect of S-516 on cell viability in prostate cancer cell lines

To determine the cell viability of S-516, we perfomred a Celltiter Glo® luminescent assay. Human prostate cancer cells (PC3, DU145, LNCaP, 22Rv1) and mouse prostate cancer cells (TRAMP-C1) were treated with 0 to 50 μmol/L S-516 for 72 hours. The concentration of S-516 was diluted in half for each experiment. As shown in Figure 1 and Table 1, S-516 inhibited the cell viability of all prostate cancer cells in a concentration-depent manner, with IC_{50} values of 0.045 μmol/L in DU145, LNCaP-0.04 μmol/L, 22Rv-0.004 μmol/L, and TRAMP-C1 0.68 μmol/L.

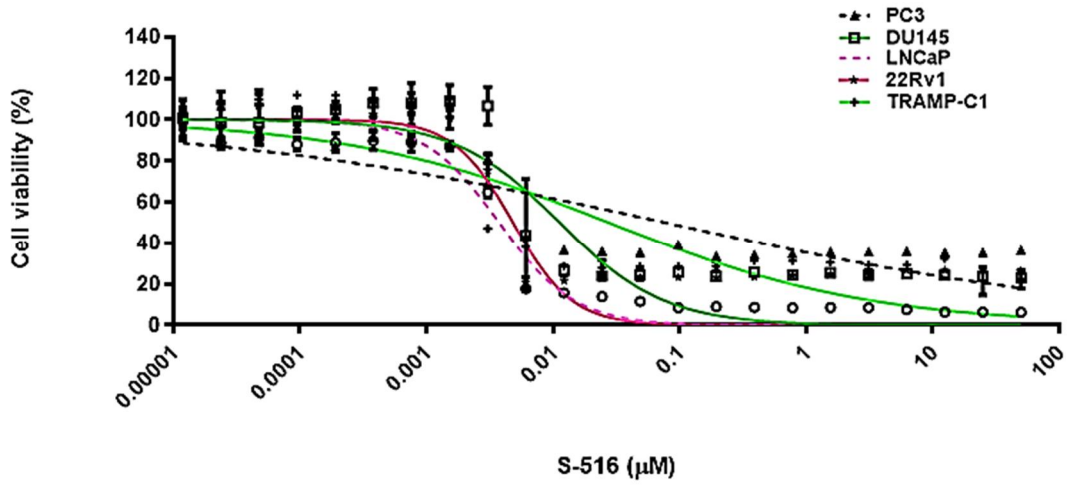

Figure 1. Effect of S-516 on cell viability in prostate cancer cells.

Human (PC3, DU145, LNCaP, 22Rv1) and mouse (TRAMP-C1) prostate cancer cells were treated with 0 to 50 μmol/L S-516 for 72 hours. Cell viability assay was determined by CellTiter GLo® luminescent assay. Results are expressed as the means ± SD of three independent experiments.

S-516 induces apoptosis in prostate cancer cell lines

Next, the potential effect of S-516 on cell apoptosis was tested. Human (PC3, DU145, LNCaP, 22Rv1) prostate cancer cells were treated with S-516 at the concentrations of IC_{50} (PC3-5 μmol/L, DU145 and LNCaP-0.04 μmol/L, 22Rv-0.004μmol/L) for 72 hours. Western blotting results in Figure 2A, treatment with S-516 significantly increased the expression of cleaved caspase-3, 9 and PARP. As shown in Figure 2B, activities of caspase-3 were significantly increased as well, followed by measuring enzyme activity using the specific synthetic substrates for caspase-3. Additionally, the quantification of apoptotic cells induced by S-516 was further calculated by flow cytometry analysis. At the dose of IC_{50} concentration, the percentage of human prostate cancer cells with positive annexin V-positive staining (apoptotic cells) was increased after S-516 treatment (Figure 2C, Table 3).

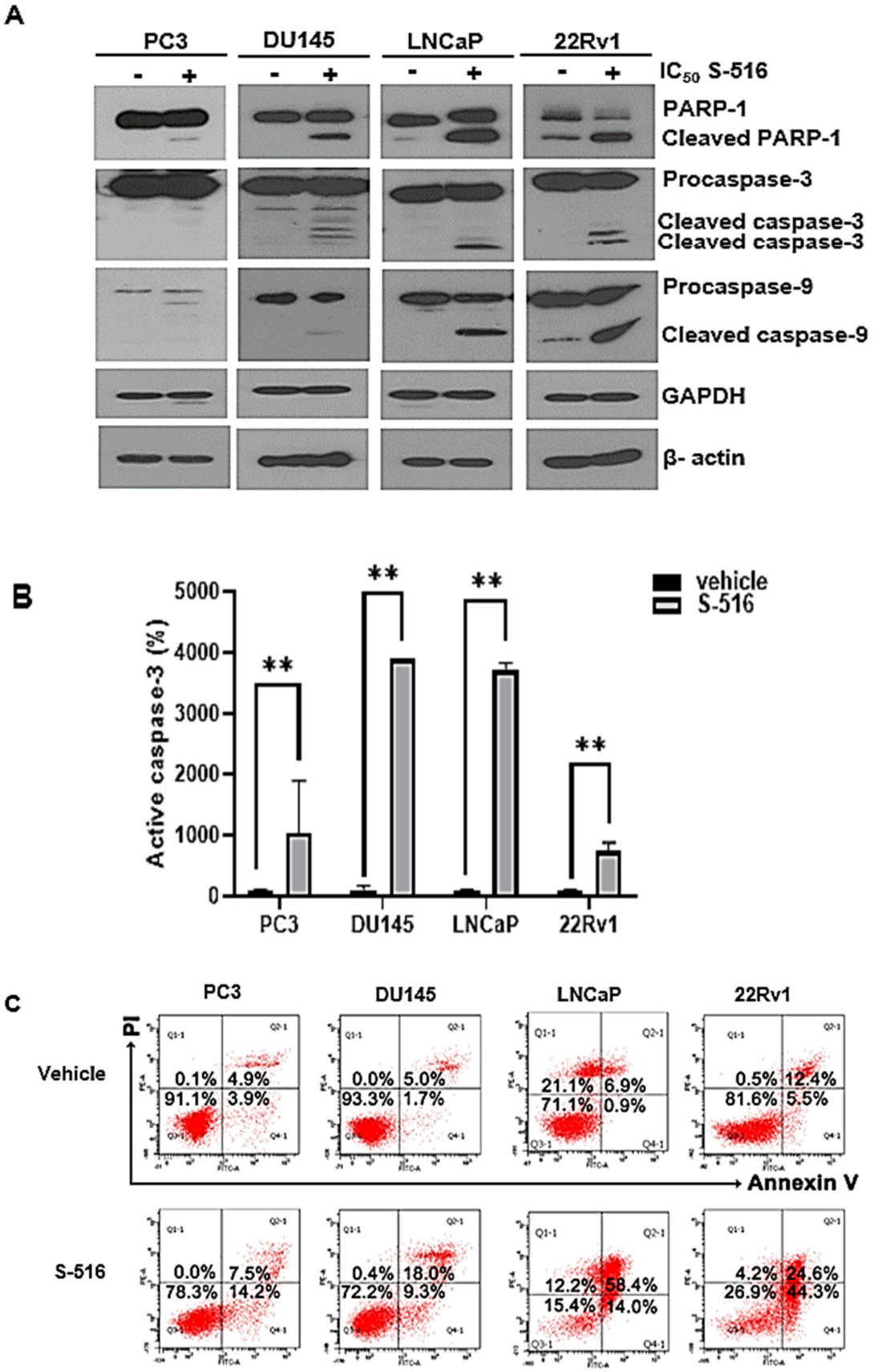
A
PC3
DU145
LNCaP
22Rv1
- + - + - + - +
IC50 S-516
PARP-1
Cleaved PARP-1
Procaspase-3
Cleaved caspase-3
Cleaved caspase-3
Procaspase-9
Cleaved caspase-9
GAPDH
β- actin
B
vehicle
S-516
Active caspase-3 (%)
5000
4000
3000
2000
1000
0
**
**
**
**
PC3
DU145
LNCaP
22Rv1
C
PC3
DU145
LNCaP
22Rv1
PI
Vehicle
0.1% 4.9%
91.1% 3.9%
0.0% 5.0%
93.3% 1.7%
21.1% 6.9%
71.1% 0.9%
0.5% 12.4%
81.6% 5.5%
Annexin V
S-516
0.0% 7.5%
78.3% 14.2%
0.4% 18.0%
72.2% 9.3%
12.2% 58.4%
15.4% 14.0%
4.2% 24.6%
26.9% 44.3%

Figure 2. Effect of S-516 on cell viability and apoptosis in prostate cancer cells.

(A) Human (PC3, DU145, LNCaP, 22Rv1) prostate cancer cells were treated with S-516 at the concentrations of IC_{50} (PC3-5 μmol/L, DU145 and LNCaP-0.04 μmol/L, 22Rv-0.004 μmol/L) for 72 hours. Western blot analysis was performed using cleaved caspase-3, cleaved caspase-9 and poly (ADP-ribose) polymerase (PARP)-1 and caspase-3 antibodies. GAPDH and β-actin were used as loading control.

(B) Bar graph demonstrating increased level of active caspase-3 in human prostate cancer cells after treatment with S-516. Active caspase-3 levels were obtained through ELISA tests.

(C) Human prostate cancer cells were treated with S-516 at the concentrations of IC_{50} for 72 hours. Flow cytometry analysis was performed by annexin-V/PI staining method. In this study, cells positive for annexin V (bottom right quadrant, Q4-1) and those positive for both annexin-V and propidium iodide (PI) (top right quadrant, Q2-1) represent the early and late apoptotic populations, respectively.

Table 3. Cell cycle distribution of human prostate cancer cells treated with S-516 for 72 hours.

(%)

	PC3		**DU145**		**LNCaP**		**22Rv1**	
	vehicle	S-516	vehicle	S-516	vehicle	S-516	vehicle	S-516
subG1	0.3	0.5	0.3	6.8	3.2	12.3	1.0	3.6
G1	70.6	15.5	60.2	9.4	66.0	23.1	39.2	22.1
S	10.9	9.4	9.6	6.4	8.7	9.4	10.6	11.9
G2	18.0	74.6	29.8	74.6	21.2	52.1	48.8	62.2

The effect of S-516 on cell cycle arrest and microtubule dynamics.

To examine whether the cell viability inhibition observed is due to cell cycle arrest followed by apoptosis, cells were treated with S-56 for 24 hours and cell cycle distribution was studied by propidium iodide (PI) flow cytometry assay. The population of cells in G2/M phase increased significantly after 24 hours of S-516 treatment. Next, we evaluated the effects of S-516 on G2/M arrest-related protein expression by western blot analysis. Cells were treated with IC_{50} concentration for 24 hours, and the expressions of Cdc2, cyclin B1, H3 and thymidine kinase I were analyzed (Figure 3B). After treatment with S-516, cells were arrested in the G2/M phase before apoptosis occurred, which were associated with upregulation of cyclin B1, dephosphorylation of Cdc2, phosphorylation of H3. Then, we assessed microtubule dynamics in S-516-treated prostate cancer cells using confocal microscopy. We treated the cells with IC_{50} concentrations of S-516, and the images acquired on confocal microscopy are shown in Figure 3C.

Microtubules are hollow tubes made up of repeating protein structures, specifically dimers of alpha and beta tubulin. Microtubules play an essential role forming mitotic spindle which is associated with cell division. Our confocal microscopy results showed that S-516 treatment caused a diffusion of red fluorescence (tubulin) in the S-516-treated cells

compared with untreated cells within 24 hours. In addition, compared to the typical cytoskeleton structures of untreated cells, which had long and dense microtubules extending throughout the cytoplasm, cells showed cellular microtubule depolymerization after 24 hours of S-516 treatment. Taken together, our results indicated that S-516 suppressed the cellular microtubule network formation by destructing the normal microtubule structure by inhibiting tubulin polymerization in prostate cancer cells.

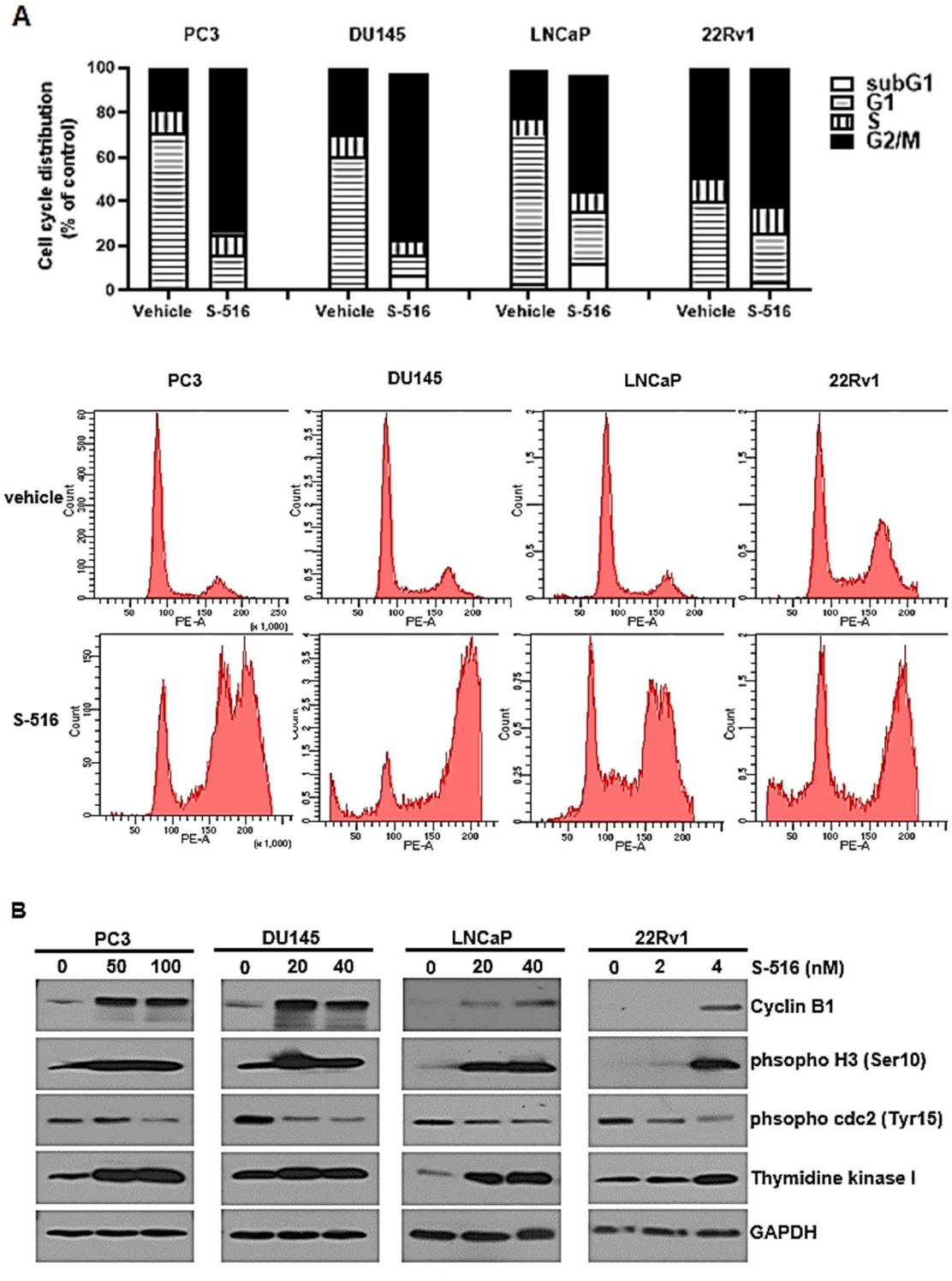
A
PC3
DU145
LNCaP
22Rv1
Cell cycle distribution (% of control)
subG1
G1
S
G2/M
Vehicle
S-516
vehicle
S-516
Count
PE-A
B
0 50 100
0 20 40
0 20 40
0 2 4
S-516 (nM)
Cyclin B1
phsopho H3 (Ser10)
phsopho cdc2 (Tyr15)
Thymidine kinase I
GAPDH

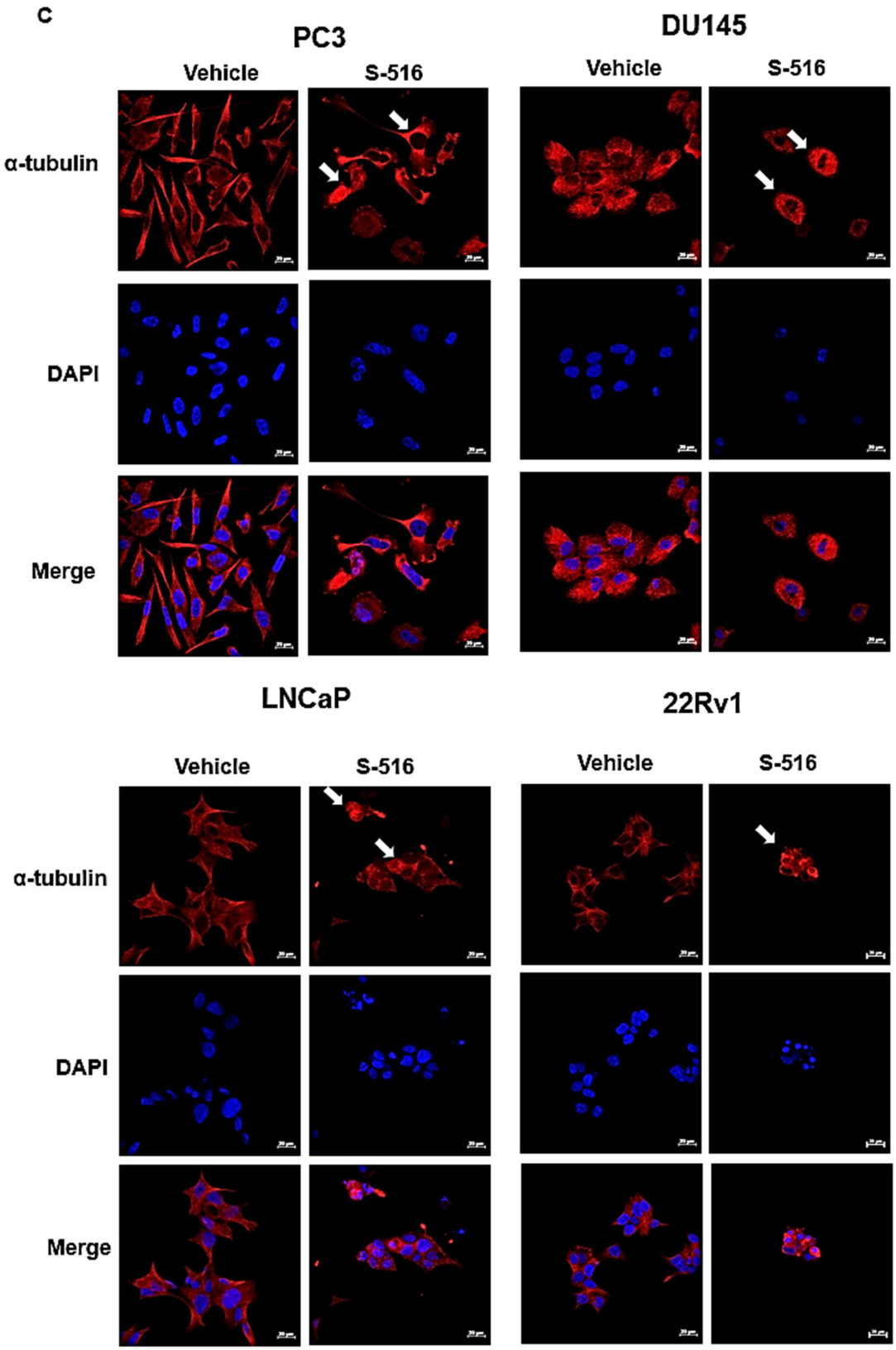
C
PC3
DU145
Vehicle
S-516
Vehicle
S-516
α-tubulin
DAPI
Merge
LNCaP
22Rv1
Vehicle
S-516
Vehicle
S-516
α-tubulin
DAPI
Merge

Figure 3. S-516 is a depolymerizing agent and caused mitotic arrest in prostate cancer cells.

(A) Human prostate cancer cells were treated IC_{50} concentration of S-516 for 24 hours in order to reach a peak of cells in G2/M arrest. Cell cycle was analyzed in parallel by flow cytometry upon PI staining. Results are presented both as a representative histogram and a chart showing the cell-cycle distribution.

(B) Human prostate cancer cells were treated IC_{50} and IC_{50} x 1/2 concentrations of S-516 for 24 hours. Western blot analysis was performed using phospho-H3 (serine 10), phospho-cdc2 (threonine 15), cyclin B1 and thymidine kinase I. GAPDH was used as loading control.

(C) Human prostate cancer cells were treated IC_{50} concentrations of S-516 for 24 hours. The changes of microtubule network were visualized by staining a-tubulin as arrows indicated. Nuclear DNA was stained by DAPI. Scale bar, 100 μM.

JNK activation plays a key role in S-516-induced apoptosis

Phosphorylation of Bcl-2 is known to suppress apoptosis and JNK induces G2/M cell cycle arrest. To investigate the mechanism of S-516 induced cell apoptosis, we analyzed the JNK signaling pathway. The results show that phosphorylation of c-JUN and JNK were induced S-516 in a concentration dependent manner (Figure 4A). In addition, we used a JNK inhibitor (SP600125) to identify the specific JNK involved in S-516-induced cell death (Figure 4B). Specific JNK inhibitor SP600125 reduced phosphorylation of Bcl-2, thus confirming a role of JNK in Bcl-2 phosphorylation (Supplementary Figure).

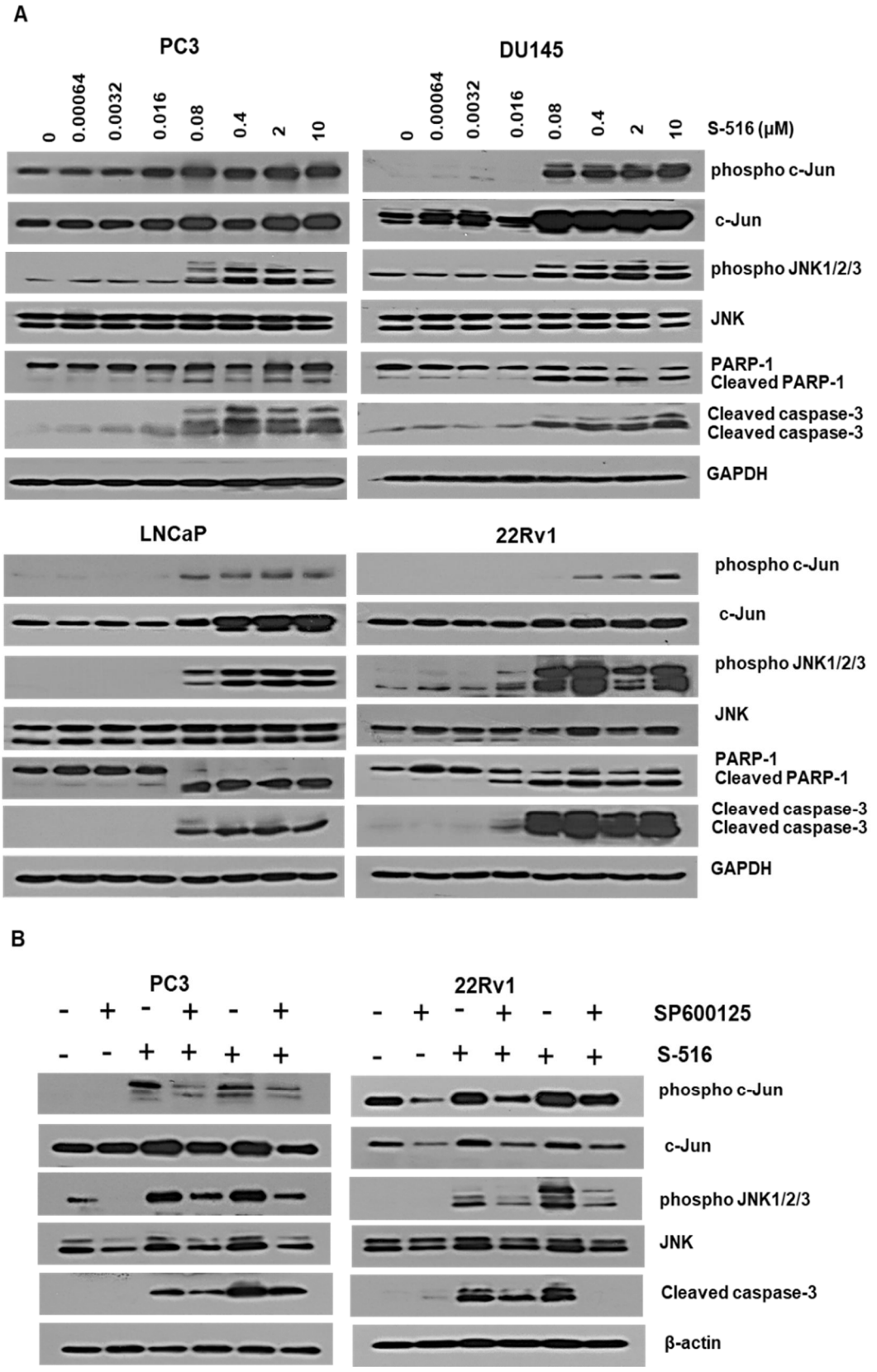
A
PC3
DU145
0
0.00064
0.0032
0.016
0.08
0.4
2
10
S-516 (μM)
phospho c-Jun
c-Jun
phospho JNK1/2/3
JNK
PARP-1
Cleaved PARP-1
Cleaved caspase-3
Cleaved caspase-3
GAPDH
LNCaP
22Rv1
B
PC3
22Rv1
SP600125
S-516
phospho c-Jun
c-Jun
phospho JNK1/2/3
JNK
Cleaved caspase-3
β-actin

Figure 4. JNK activation was involved in S-516-induced cell apoptosis

(A) Human prostate cancer cells were treated with indicated concentration of S-516 for 72 hours. Western blot analysis was performed using phospho JNK1 (threonine 183)+JNK2 (threonine 183)+JNK3 (threonine 221), JNK1/2/3, phospho c-JUN (serine 73), phospho Bcl-2, Bcl-2, cleaved caspase-3 and PARP-1 antibodies. GAPDH was used as loading control.

(B) Cells were pre-incubated for 30 min with JNK inhibitor, SP600125, alone or in combination and then treated for 48 hours with S-516 at the concentrations of IC_{50}. Western blot analysis performed using phospho JNK1 (threonine 183)+JNK2 (threonine 183)+JNK3 (threonine 221), JNK1/2/3, phospho c-JUN (serine 73), phospho Bcl-2 and Bcl-2 antibodies. GAPDH was used as loading control.

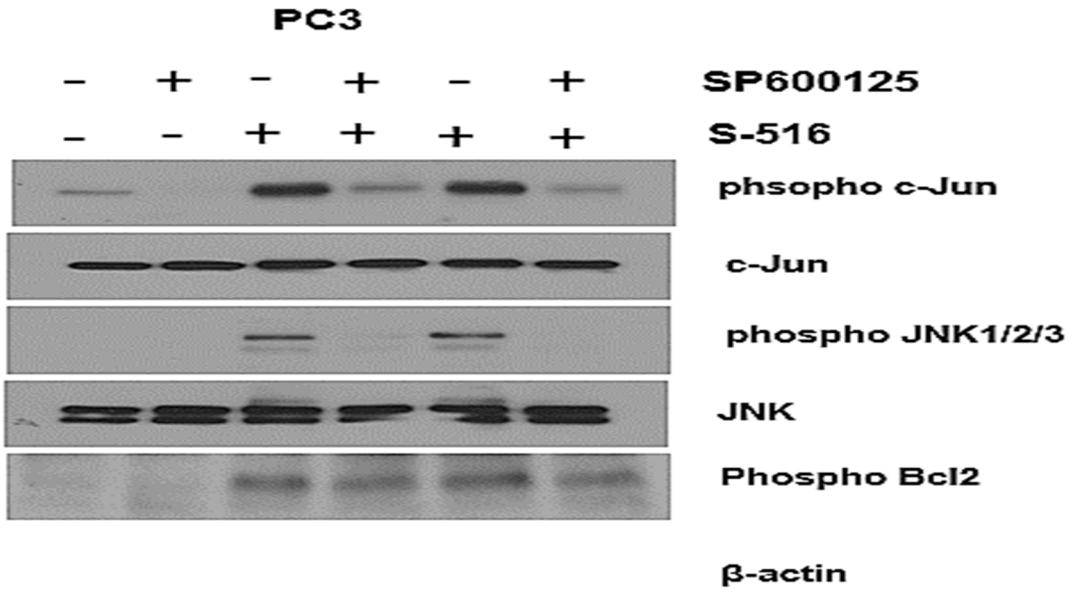

Supplementary figure. The role of JNK in Bcl-2 phosphorylation. β-actin was used as loading control.

CKD-516 synergizes with PD-1 blockade through enhancing antitumor immunity

In vivo efficacy of CKD-516 in combination with anti-PD-1 antibody was evaluated in a syngeneic TRAMP-C1 mouse model. Cells were implanted subcutaneously ito C57BL/6 mice. When tumor volumes reached at least 50-70 mm^3, mice were treated with either anti-PD-1 antibody or CKD-516 or both. Treatment frequency was twice a week with 3-week period.(Figure 5A) Tumor volume was measured every 2 to 3 days. All of the mice gradually gained body weight which indicates the feasiblity of the experiment (Figure 5D). We found that at day 57 of treatement, while monotherapy with CKD-516 3mg/kg/day, 6mg/kg/day or anti-PD-1 antibody moderately reduced tumor volume with tumor growth inhibition (TGI) of 34.64%, 38.02% and 40.92%, respectively, combination treatement demonstrated significantly greater antitumor efficacy with TGI of 90.69% in CKD-516 3mg/kg/day+anti-PD-1 5mg/kg/day and 90.7% in CKD-516 3mg/kg/day+anti-PD-1 5mg/kg/day.(Table 4)

Table 4. Synergistic effect of combination therapy with CKD-516 and PD-1 antibody.

Group	Tumor growth inhibition(%)
CKD-516(3mg/kg)	34.64
CKD-516(6mg/kg)	38.02
PD-1 antibody(5mg/kg)	40.92
CKD-516(3mg/kg)+PD-1 antibody(5mg/kg)	90.69
CKD-516(6mg/kg)+PD-1 antibody(5mg/kg)	90.7

At the end of the experiments, all tumor were extracted for volume measurement.(Figure 5C) The combination therapy dominantly decreased the tumor volume and weight.(Figure 5C, 5E) Cleaved caspase-3 was detected more after the combination therapy.(Figure 5F)

To examine the mechanism of the synergistic antitumor effects of combined PD-1 blockade and tubulin polymerization inhibition, we investigated on the immunological response of mice. Spleen of the mice were resected to estimate the IFN-γ secretion to evaluate the immunological response. ELISA tests confirmed the relative IFN-γ concentration.(Figure 6A) The concentration was significantly increased after treatment with CKD-516 or anti-PD-1. Figure 6B demonstrates the results of ELISpot which visualizes the secretion of IFN-γ. Anti-PD-1 antibody treatment and the combination therapy with CKD-516 showed favorable secretion of IFN-γ.

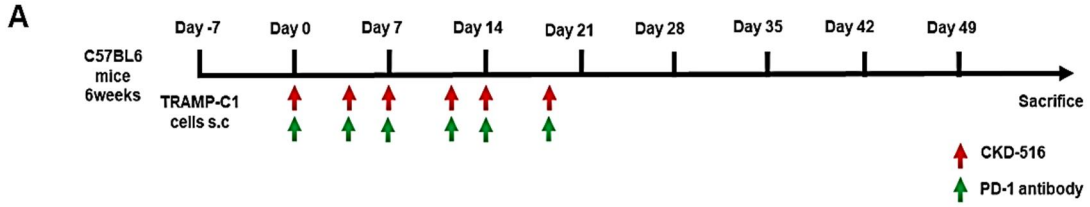
A
Day -7
Day 0
Day 7
Day 14
Day 21
Day 28
Day 35
Day 42
Day 49
C57BL6
mice
6weeks
TRAMP-C1
cells s.c
Sacrifice
CKD-516
PD-1 antibody

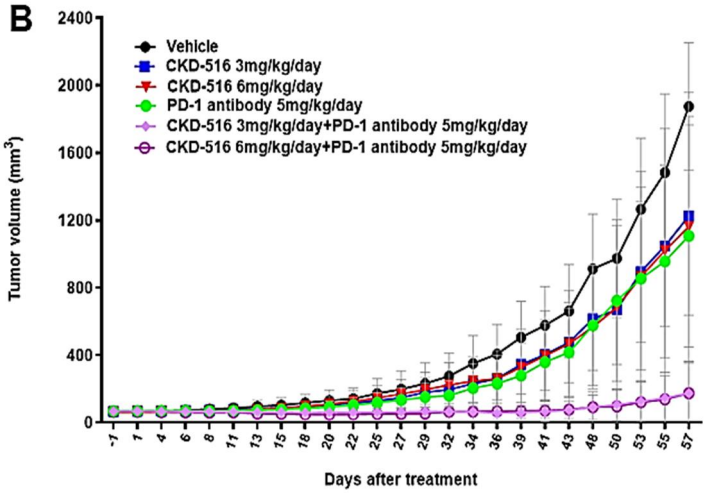
B
Vehicle
CKD-516 3mg/kg/day
CKD-516 6mg/kg/day
PD-1 antibody 5mg/kg/day
CKD-516 3mg/kg/day+PD-1 antibody 5mg/kg/day
CKD-516 6mg/kg/day+PD-1 antibody 5mg/kg/day
Tumor volume (mm3)
Days after treatment

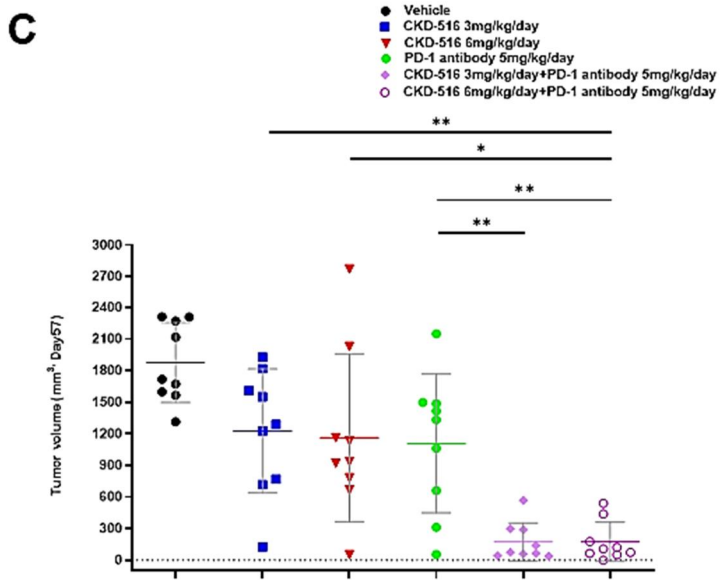
C
Vehicle
CKD-516 3mg/kg/day
CKD-516 6mg/kg/day
PD-1 antibody 5mg/kg/day
CKD-516 3mg/kg/day+PD-1 antibody 5mg/kg/day
CKD-516 6mg/kg/day+PD-1 antibody 5mg/kg/day
Tumor volume (mm3, Day57)

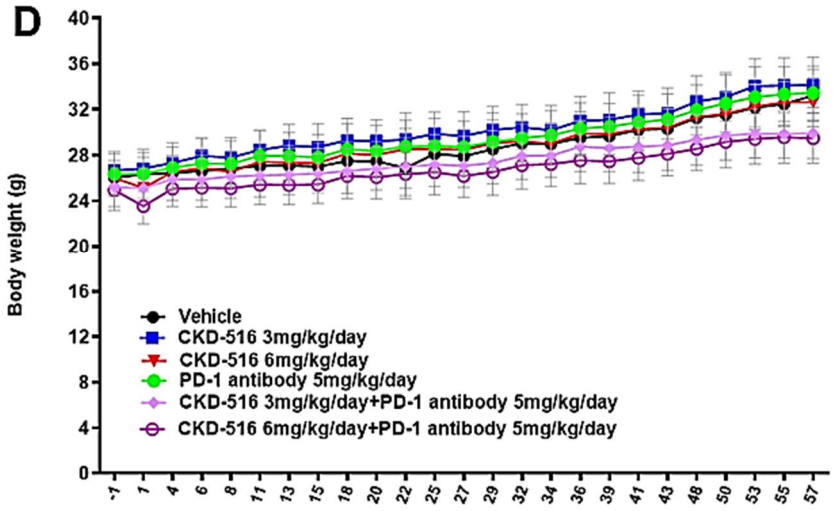
D
Body weight (g)
40
36
32
28
24
20
16
12
8
4
0
-1
1
4
6
8
11
13
15
18
20
22
25
27
29
32
34
36
39
41
43
48
50
53
55
57
Vehicle
CKD-516 3mg/kg/day
CKD-516 6mg/kg/day
PD-1 antibody 5mg/kg/day
CKD-516 3mg/kg/day+PD-1 antibody 5mg/kg/day
CKD-516 6mg/kg/day+PD-1 antibody 5mg/kg/day

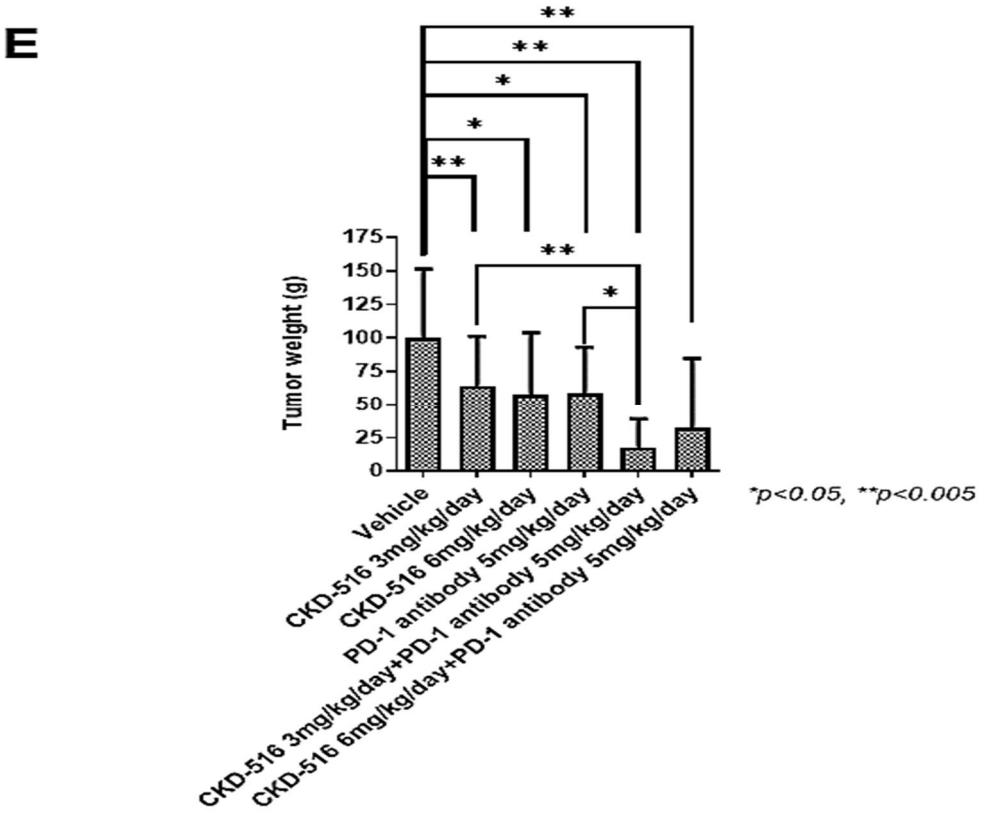
E
Tumor weight (g)
175
150
125
100
75
50
25
0
**
**
*
*
**
**
*
*p<0.05, **p<0.005
Vehicle
CKD-516 3mg/kg/day
CKD-516 6mg/kg/day
PD-1 antibody 5mg/kg/day
CKD-516 3mg/kg/day+PD-1 antibody 5mg/kg/day
CKD-516 6mg/kg/day+PD-1 antibody 5mg/kg/day

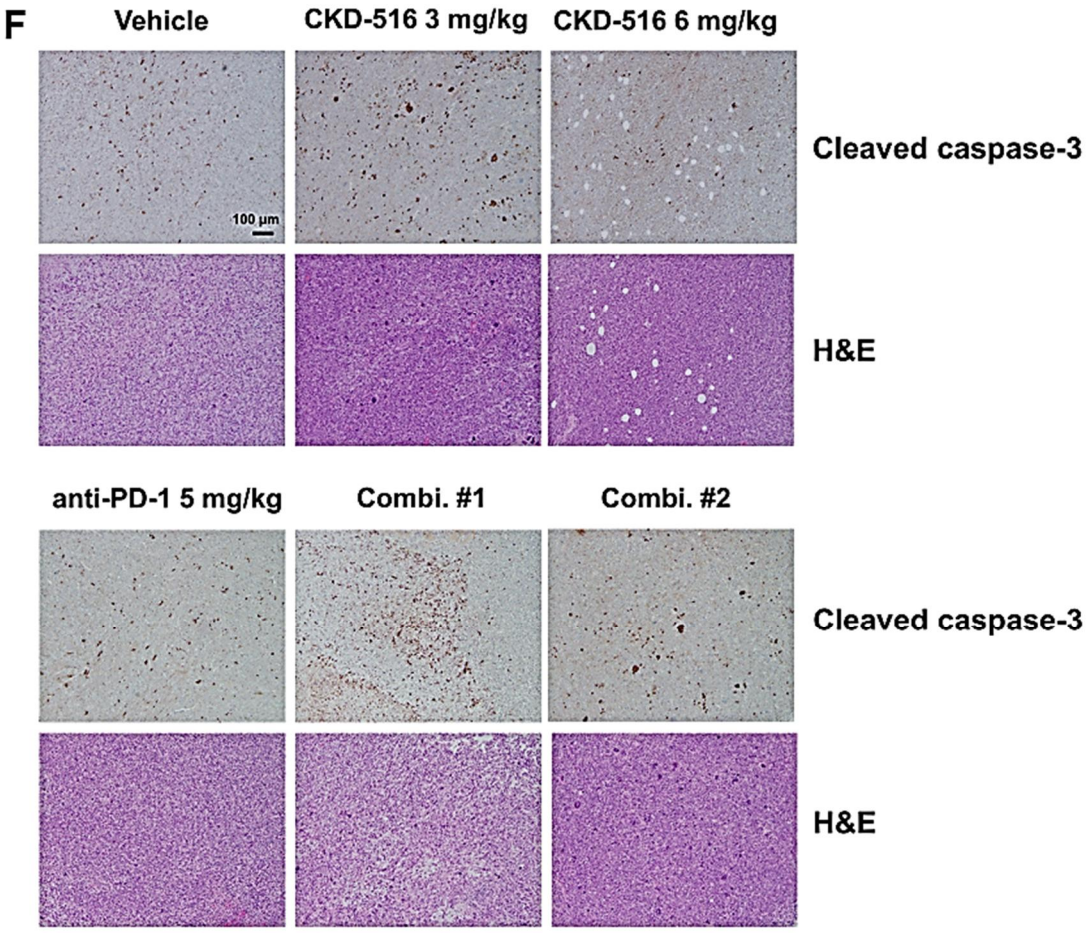

Figure 5. Anti-tumor efficacy of treatment with CKD-516 alone or in combination with *anti*-PD-1.

Male C57BL/6 mice were implanted with 5 x 10^6 cells TRAMP-C1 cells subcutaneously and received one of 6 treatments: Vehicle (control antibody treatment/purified water), 3mg/kg CKD-516, 6mg/kg CKD-516, 5 mg/kg *anti*-PD-1, or *anti*-PD-1 plus 3mg/kg CKD-516, or *anti*-PD-1 plus 6mg/kg CKD-516. Drugs were administered twice per week for 3 weeks.

(A) Schematic of the treatment plan for mice bearing subcutaneous TRAMP-C1 tumors.

(B) Changes in tumor volume. Results are expressed as the means ± SD of TRAMP-C1 syngeneic mouse model.

(C) End-point tumor volume at the day 57. Results are expressed as the means ± SD of TRAMP-C1 tumors.

(D) Changes in body weight. Results are expressed as the means ± SD of TRAMP-C1 syngeneic mouse model.

(E) Tumor weight. Results are expressed as the means ± SD of TRAMP-C1 tumors.

(F) TRAMP-C1 tumors were resected and the sections were analyzed by immuno-histochemistry using cleaved caspase-3 antibodies. Representative photographs are shown. Scale bar, 100 μM. (Combi #1; anti-PD-1 5mg/kg plus CKD-516 3mg/kg, Combi #2; anti-PD-1 5mg/kg plus CKD-516 6mg/kg)

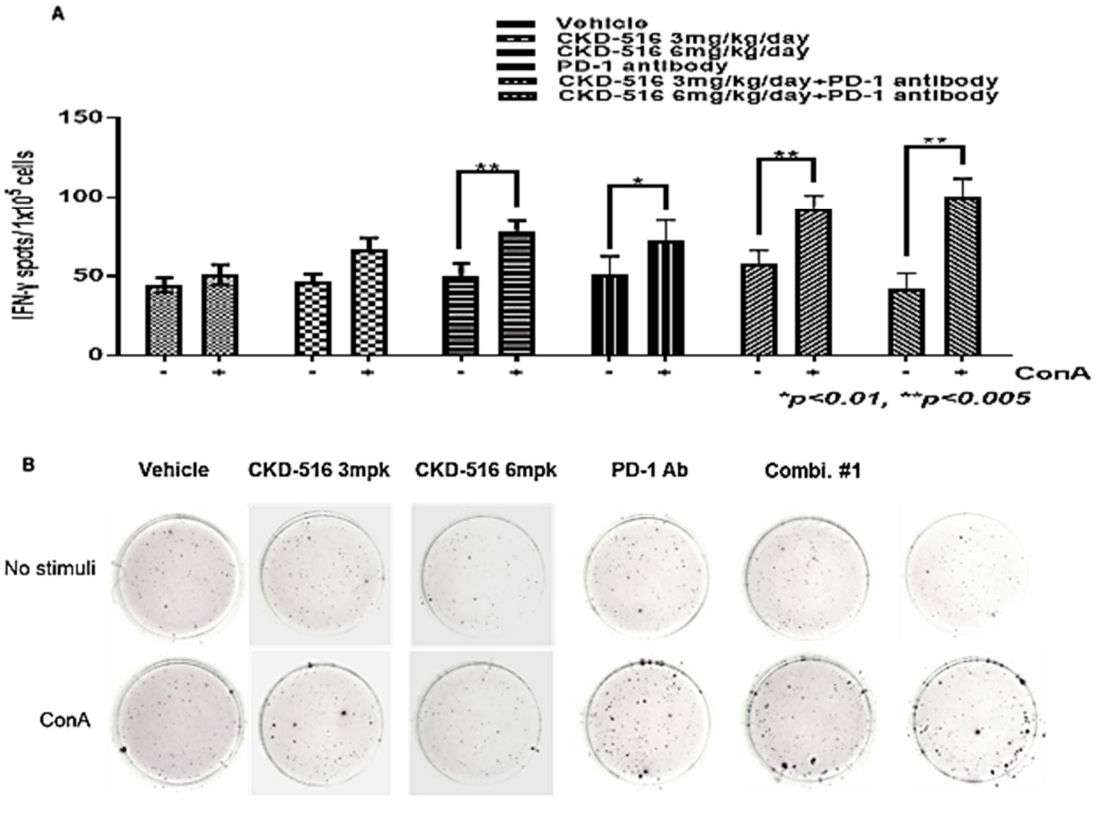

Figure 6. The mechanism of anti-tumor immune response.

Vehicle or treated mice were euthanized 57 days after the initiation of the treatment, splenocytes were harvested and ELISPOT assay and ELISA assay were performed.

(A) Combination of CKD-516 and *anti*-PD-1 on the effects of INF-γ levels from spleen in TRAMP-C1-bearing mice. The mouse spleens were harvested at the ends of experiment (day 57) and stimulated with LPS. The increase in INF-γ levels in spleen was observed in five treatment groups compared with the vehicle group (untreated LPS). Results are expressed as the means ± SD, compared with vehicle group.

(B) Tumor antigen-specific alterations in immunological parameters were analyzed with splenic lymphocytes obtained from the TRAMP-C1 tumor bearing mice treat CKD-516 and

anti-PD-1. The cytotoxic T lymphocytes(CTLs) were stimulated with the use of stimulated-concanavalin A(ConA). The proportion of INF-γ-secreting CD8+ T cells was observed by ELISpot assay (lower panel). The relative mean numbers of spots compared with the vehicle group (untreated concanavalin A) are shown (upper panel).

The effect of S-516 on Dendritic cell maturation

C57BL/6 mouse DCs (mDC) were used for the experiments. mDCs were treated with indicated concentration (50, 100, 200nM) of S-516 for 24 hours.(Figure 7A) As the concentration of S-516 increases, the amount of mDC significantly increased.(Figure 7B) Western blot analysis was performed using phospho JNK1(threonine 183)+JNK2 (threonine 183)+JNK3 (threonine 221), phospho c-JUN (serine73) and c-JUN antibodies to confirm the activation of mDC maturation pathway.(Figure 7C) Increase in relative protein expressions was definite in all proteins more predominantly in p-JNK/JNK. Expression of surface marker CD80 and CD86 was increased with S-516 treatment.(Figure 7D) However, the surface markers of DC was not dose dependent to S-516.

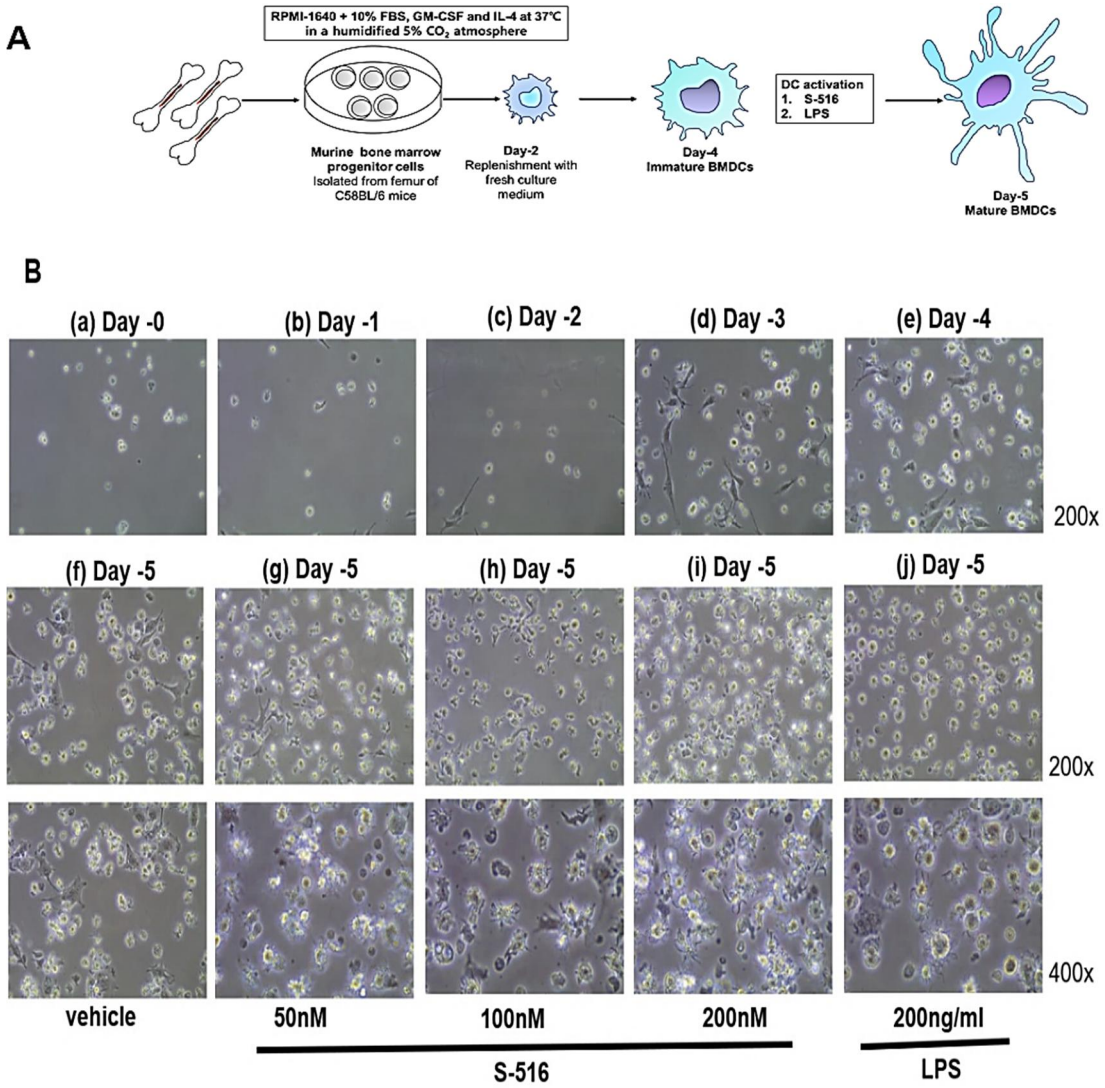
A
RPMI-1640 + 10% FBS, GM-CSF and IL-4 at 37°C
in a humidified 5% CO2 atmosphere
Murine bone marrow progenitor cells
Isolated from femur of C58BL/6 mice
Day-2
Replenishment with fresh culture medium
Day-4
Immature BMDCs
DC activation
1. S-516
2. LPS
Day-5
Mature BMDCs
B
(a) Day -0
(b) Day -1
(c) Day -2
(d) Day -3
(e) Day -4
200x
(f) Day -5
(g) Day -5
(h) Day -5
(i) Day -5
(j) Day -5
200x
400x
vehicle
50nM
100nM
200nM
200ng/ml
S-516
LPS
C
S-516 (nM)
-
50
100
200
LPS
phospho JNK1/2/3 (Thr183/Thr221)
JNK
phospho c-JUN (Ser73)
c-JUN
GAPDH
Relative protein expression (% of control)
1500
1000
500
400
300
200
100
0
vehicle
50 nM
100 nM
200 nM
LPS
S-516
p-JNK/JNK
p-c-JUN/c-JUN

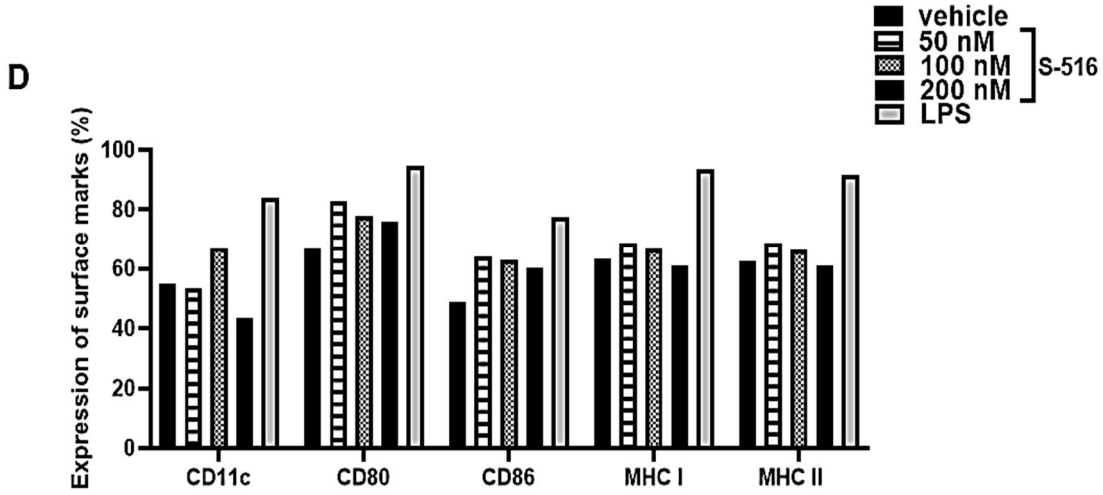

Figure 7. Dendritic cell maturation via S-516.

(A) Schema demonstrating the maturation of bone marrow dendritic cells(BMDCs). Bone marrow-derived DCs (BMDCs) were induced from bone marrow (BM) cells obtained from specific pathogen-free female C57BL/6 mice. Cells were isolated from the BM cells and cultured with GM-CSF and IL-4 (1 x 103 units/ml each) at 37□ for 4 days in a humidified CO^2 incubator for monocyte-derived dendritic cells differentiation. BMDCs maturation was activated by known DC activator lipopolysaccharide(LPS) and S-516.

(B) Bone marrow cells are cultured in growth medium RPMI-1640 with 10% FBS containing 1,000 unit/ml rmGM-CSF and rmIL-4 for 7 days. Fresh medium is supplemented at day-2. (a) Bone marrow precursors at day-0, (b) day-1 Monocyte-Derived Dendritic cells(MoDCs), (c) day-2 MoDCs (d) day-3 MoDCs (e) day-4 MoDCs (f1-5) day-5 immature MoDCs-untreated and treated with maturation stimulus LPS (50ug/ml) and S-516 (50, 100, 200nM) for 24h.

(C) C57BL/6 mouse DCs (mDC) were used for the experiments. DCs were treated with indicated concentration (50, 100, 200 nM) of S-516 for 24 hours. Western blot analysis was performed using phospho JNK1 (threonine 183)+JNK2 (threonine 183)+JNK3 (threonine 221), phospho c-JUN (serine73) and c-JUN antibodies. GAPDH was used as loading control.

(D) C57BL/6 mouse DCs (mDC) were used for the experiments. DCs were treated with indicated concentration (50, 100, 200 nM) of S-516 for 24 hours. Expressions of CD80 and CD86 detected by flow cytometry.

Discussion

CKD-516, a novel VDA, was proved to be efficient in human prostate cancer cells in our study. Figure 8A shows theoretical flow of antitumor mechanisms of CKD-516.

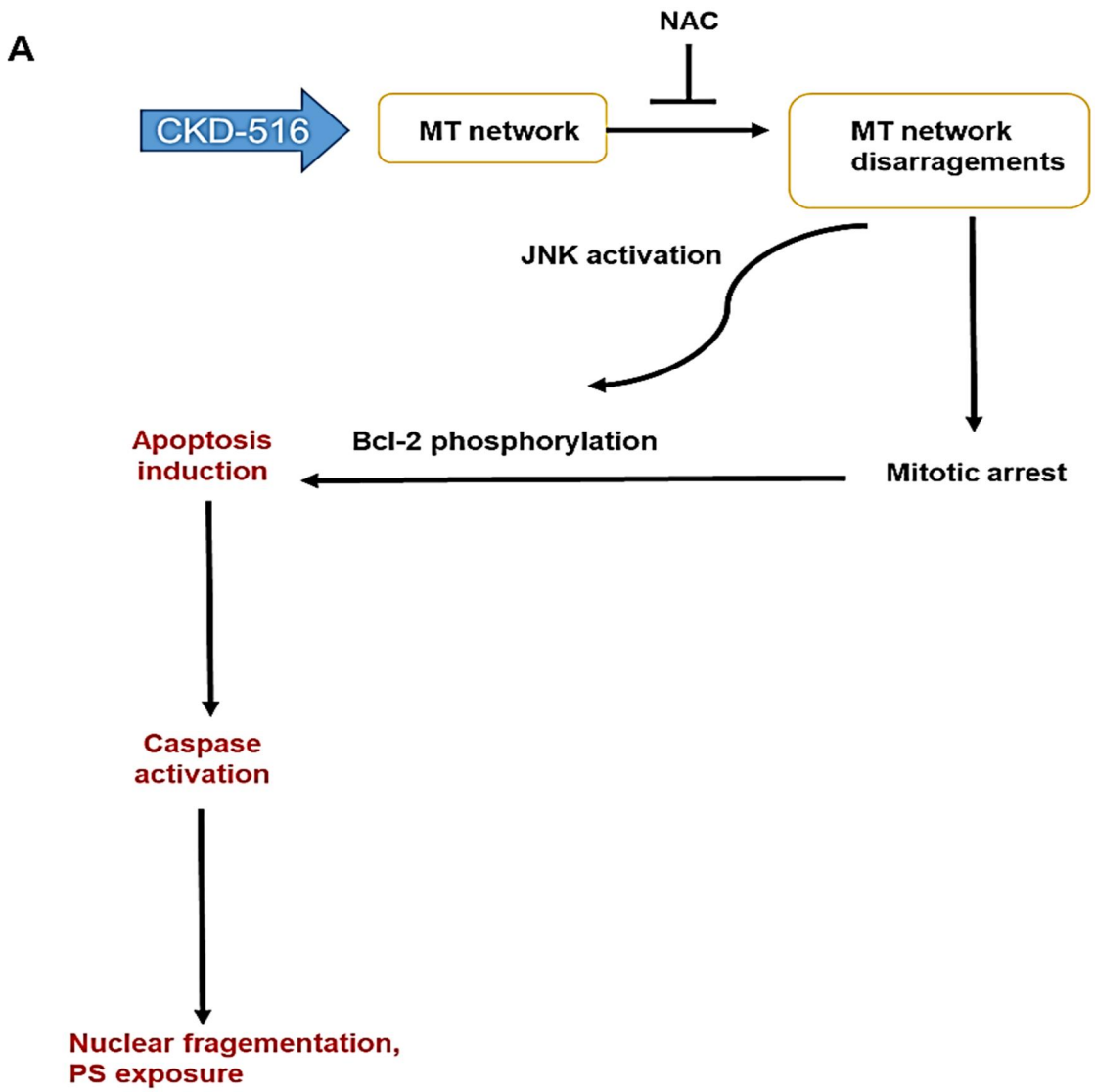

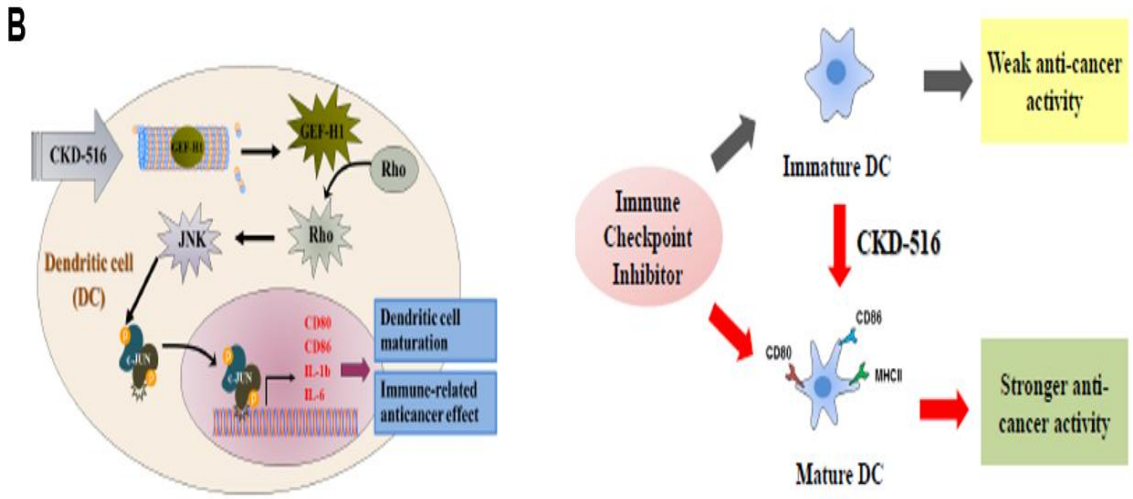

Figure 8. Antitumor mechanisms of CKD-516.

(A) CKD-516 induced apoptosis via JNK activation and mitotic arrest

(B) CKD-516 directly induced DC maturation.

When it is administered, mitochondrial network of the cells starts to disarrange which leads to mitotic arrest and JNK activation. Then Bcl-2 phosphorylation occurs which initiates caspase activation and apoptosis induction. This makes nuclear fragmentation and phosphatidylserine exposure and finally induce cell death. In this study, we apparently demonstrated that S-516 induces c-JUN and JNK activation(Figure 4A). Furthermore, c-JUN, JNK activation pathway was confirmed by treating cells with JNK inhibitor SP600125. After SP600125 administration, phopho c-JUN, phospho-JNK1/2/3 was inhibited.(Figure 4B) This mechanism was similar with

a novel synthetic quinolone derivative MPT0B392(B392) which was used against acute leukemia.[17] B392 stimulated the induction of the mitotic arrest, followed by mitochondrial membrane potential loss and caspases cleavage by activation of c-JUN, JNK pathway. After the activation of this pathway, B392 demonstrated therapeutic effect in drug resistant cancer cells. Therefore, like B392, CKD-516 was thought to have therapeutic effect in tumors and it was clearly proved by detecting the mitotic arrest(Figure3A) and reduced tumor volume(Figure5C). We also demonstrated the potential antitumor effect of combining PD-1 inhibitor with CKD-516 and combination therapy was superior compared to single use of therapeutic agents.(Figure 5B)

Dendritic cells (DCs) are potent antigen-presenting cells (APCs), which plays a critical role in inducing, maintaining and regulating T-cell responses.[18, 19] In tumors, DCs circulate through the blood vessels and migrate toward tumor tissues, in which they interact with tumor cells. Immature DCs are efficient in uptaking tumor-derived materials. DC maturation is induced by tumor-derived materials as well as proinflammatory cytokines produced by various tumor-infiltrating immune cells.[20] Apart from their outstanding ability to induce and control T-cell responses, matured DCs efficiently improve the immunomodulatory and cytotoxic potential of natural killer cells, which essentially eliminates tumor cells.[21, 22] However, without these mechanisms, S-516 significantly induced DC maturation even more effectively than known DC activator LPS.(Figure 7B) Owing to its antitumor effects throughout the DC

maturation, S-516 could be a promising agent for various cancers including prostate cancer.

VDAs have demonstrated their clinical potential as antitumor agents in many pre-clinical research and some of these are currently being investigated in clinical trials. Although VDAs bring about an extensive central necrosis, a periphery of tumors still remain[23], from which tumor regrowth initiates. The treatment failure of such agents to target the peripheral tumor rim means that their efficacy as a single therapeutic agent is not enough.[24] Previous studies have suggested that anti-angiogenic therapy including VDAs can enhance tumor immunity response and conversely, the immune system can provoke angiogenesis.[25-27] Horsman et al.[28] demonstrated that mammary carcinoma which was unresponsive to immune checkpoint inhibitors became responsive in mice treated with VDAs. These results gives rationale to the use of VDAs in combination with other therapeutic agents including immune checkpoint inhibitor which might have potential to overcome the treatment resistant cancer cells. Our study results demonstrate the potential of VDAs to convert immunological insensitive tumors into ones that were immunologically sensitive and this may have clinical importance.(Figure 8B) Many VDAs are in clinical evaluations[29] but whether the therapeutic effects seen with these combretastatin drugs is a general phenomenon for all VDAs is not precisely known. Thus it is certainly valuable work to conduct further investigations.

Oh et al. has shown that intravenous injection of CKD-516 had a manageable safety

profile in patients with solid tumors.[29] After this study, Kim et al. successfully reported that an oral from of CKD-516 was tolerable in patients with refractory solid tumors without noticable increase in drug toxicity. [30] Diarrhea was the most common grade 3 toxicity associated with intravenous and oral administration of CKD-516. Grade 2 or grade 3 nausea presented in 30% of the enrolled patients in these studies but was tollerable with serotonin antagonists and minimal dose of steroids. In addition, CKD-516 demonstrated no serious cardiovascular adverse events that were reported with administration of other VDAs.[31, 32] Although our study was not a clinical study, it demonstrated no serious adverse event with oral administration of CKD-516 in mice. These evidences strengthen the feasibility to perform further clinical reseach in patients with treatment resistant advanced prostate cancer.

Up to recently, many clinical studies are undergoing to test the impact of inhibition of angiogenesis and immune checkpoints. The preliminary results are positive and initial phase I/II data reported the superiority of combined treatment compared to monotherapy. To our knowledge, this is the first study in field of advanced prostate cancer suggesting that combination therapy with immune checkpoint inhibitor and CKD-516 is an effective treatment strategy.

Conclusions

A novel VDA CKD-516 is a safe, efficient antitumor agent that can play a vital role in controlling advanced prostate cancer. Combination therapy with anti-PD-1 could provide better treatment outcome. Further clinical studies must verify our results

References

1. Bray, F., et al., *Global cancer statistics 2018: GLOBOCAN estimates of incidence and mortality worldwide for 36 cancers in 185 countries.* CA Cancer J Clin, 2018. **68**(6): p. 394-424.

2. Kalmuk, J., et al., *Multimodal imaging guided preclinical trials of vascular targeting in prostate cancer.* Oncotarget, 2015. **6**(27): p. 24376-92.

3. Gustavsson, H., K. Welen, and J.E. Damber, *Transition of an androgen-dependent human prostate cancer cell line into an androgen-independent subline is associated with increased angiogenesis.* Prostate, 2005. **62**(4): p. 364-73.

4. Moon, C.H., et al., *CKD-516 displays vascular disrupting properties and enhances anti-tumor activity in combination with chemotherapy in a murine tumor model.* Invest New Drugs, 2014. **32**(3): p. 400-11.

5. Hollebecque, A., C. Massard, and J.C. Soria, *Vascular disrupting agents: a delicate balance between efficacy and side effects.* Curr Opin Oncol, 2012. **24**(3): p. 305-15.

6. Kim, S.J., et al., *Involvement of ER stress and reactive oxygen species generation in anti-cancer effect of CKD-516 for lung cancer.* Cancer Chemother Pharmacol, 2020. **85**(4): p. 685-697.

7. Ji, Y.T., Y.N. Liu, and Z.P. Liu, *Tubulin colchicine binding site inhibitors as vascular*

disrupting agents in clinical developments. Curr Med Chem, 2015. **22**(11): p. 1348-60.

8. Moon, C.H., et al., *KML001 displays vascular disrupting properties and irinotecan combined antitumor activities in a murine tumor model.* PLoS One, 2013. **8**(1): p. e53900.

9. Lee, J., et al., *Identification of CKD-516: a potent tubulin polymerization inhibitor with marked antitumor activity against murine and human solid tumors.* J Med Chem, 2010. **53**(17): p. 6337-54.

10. Scher, H.I., et al., *Increased survival with enzalutamide in prostate cancer after chemotherapy.* N Engl J Med, 2012. **367**(13): p. 1187-97.

11. Ryan, C.J., et al., *Abiraterone in metastatic prostate cancer without previous chemotherapy.* N Engl J Med, 2013. **368**(2): p. 138-48.

12. Kawalec, P., et al., *Sipuleucel-T immunotherapy for castration-resistant prostate cancer. A systematic review and meta-analysis.* Arch Med Sci, 2012. **8**(5): p. 767-75.

13. Parker, C., et al., *Alpha emitter radium-223 and survival in metastatic prostate cancer.* N Engl J Med, 2013. **369**(3): p. 213-23.

14. de Bono, J.S., et al., *Prednisone plus cabazitaxel or mitoxantrone for metastatic castration-resistant prostate cancer progressing after docetaxel treatment: a randomised open-label trial.* Lancet, 2010. **376**(9747): p. 1147-54.

15. Tannock, I.F., et al., *Docetaxel plus prednisone or mitoxantrone plus prednisone for advanced prostate cancer.* N Engl J Med, 2004. **351**(15): p. 1502-12.

16. Fay, A.P. and E.S. Antonarakis, *Blocking the PD-1/PD-L1 axis in advanced prostate cancer: are we moving in the right direction?* Ann Transl Med, 2019. **7**(Suppl 1): p. S7.

17. Chao, M.W., et al., *An oral quinoline derivative, MPT0B392, causes leukemic cells mitotic arrest and overcomes drug resistant cancer cells.* Oncotarget, 2017. **8**(17): p. 27772-27785.

18. Banchereau, J., et al., *Immunobiology of dendritic cells.* Annu Rev Immunol, 2000. **18**: p. 767-811.

19. Steinman, R.M. and J. Banchereau, *Taking dendritic cells into medicine.* Nature, 2007. **449**(7161): p. 419-26.

20. Jahnisch, H., et al., *Dendritic cell-based immunotherapy for prostate cancer.* Clin Dev Immunol, 2010. **2010**: p. 517493.

21. Fernandez, N.C., et al., *Dendritic cells directly trigger NK cell functions: cross-talk relevant in innate anti-tumor immune responses in vivo.* Nat Med, 1999. **5**(4): p. 405-11.

22. Wehner, R., et al., *Reciprocal activating interaction between 6-sulfo LacNAc+ dendritic cells and NK cells.* Int J Cancer, 2009. **124**(2): p. 358-66.

23. Taylor, M., et al., *Reversing resistance to vascular-disrupting agents by blocking late*

mobilization of circulating endothelial progenitor cells. Cancer Discov, 2012. **2**(5): p. 434-49.

24. Kanthou, C. and G.M. Tozer, *Microtubule depolymerizing vascular disrupting agents: novel therapeutic agents for oncology and other pathologies.* Int J Exp Pathol, 2009. **90**(3): p. 284-94.

25. Vanneman, M. and G. Dranoff, *Combining immunotherapy and targeted therapies in cancer treatment.* Nat Rev Cancer, 2012. **12**(4): p. 237-51.

26. Tartour, E., et al., *[Cancer immunotherapy: recent breakthroughs and perspectives]*. Med Sci (Paris), 2011. **27**(10): p. 833-41.

27. Topalian, S.L., C.G. Drake, and D.M. Pardoll, *Immune checkpoint blockade: a common denominator approach to cancer therapy.* Cancer Cell, 2015. **27**(4): p. 450-61.

28. Horsman, M.R., et al., *Tumors Resistant to Checkpoint Inhibitors Can Become Sensitive after Treatment with Vascular Disrupting Agents.* Int J Mol Sci, 2020. **21**(13).

29. Oh, D.Y., et al., *Phase I Study of CKD-516, a Novel Vascular Disrupting Agent, in Patients with Advanced Solid Tumors.* Cancer Res Treat, 2016. **48**(1): p. 28-36.

30. Kim, H.K., et al., *Phase I and pharmacokinetic study of the vascular-disrupting agent CKD-516 (NOV120401) in patients with refractory solid tumors*. Pharmacol Res Perspect, 2020. **8**(2): p. e00568.

31. Grisham, R., et al., *Clinical trial experience with CA4P anticancer therapy: focus on efficacy, cardiovascular adverse events, and hypertension management.* Gynecol Oncol Res Pract, 2018. **5**: p. 1.

32. Sessa, C., et al., *Phase I safety, pharmacokinetic and pharmacodynamic evaluation of the vascular disrupting agent ombrabulin (AVE8062) in patients with advanced solid tumors.* Clin Cancer Res, 2013. **19**(17): p. 4832-42.

국문요약

연구목적: CKD-516 은 새롭게 개발된 혈관 저해제이다. 본 연구에서는 전립선암 세포주 및 동물 모델에서 CKD-516 의 항암 효과와 기전을 조사하였다. 또한 CKD-516 과 면역관문 억제제 병용 요법의 시너지 효과를 조사하였다.

연구 방법: CKD-516 의 활성 대사 산물인 S-516 을 시험관 내 연구에 사용하였다. 마우스 전립선 상피 선암 세포주 TRAMP-C1 과 PC3, DU145, LNCaP 및 22Rv1 을 포함하는 인간 전립선암 세포주를 실험에 사용하였다. 세포 생존력 분석을 수행하였고 CKD-516 의 기전을 웨스턴 블롯 분석으로 확인하였다. 생체 내 분석을 위해 TRAMP-C1 세포를 실험용 마우스에 이식하고 CKD-516 을 3mg / kg 또는 6mg / kg 으로 3 주 동안 주 2 회 경구 위관 영양법을 통해 투여하였다. 병용 요법 연구를 위해 PD-1 항체는 3 주 동안 주 2 회 5mg / kg 의 농도로 주사하였다. 수지상세포에 대한 CKD-516 의 성숙 효과를 확인하기 위해 수지상 세포를 배양하였다.

연구결과: S-516 은 IC_{50} 값이 DU145 에서 0.045 μmol / L, LNCaP 에서 0.04 μmol / L, 22Rv1 에서 0.004 μmol / L, 그리고 TRAMP-C1 에서 0.68 μmol 였으며 농도 의존적 방식으로 모든 전립선암 세포의 생존력을 억제하였다. S-516 은 c-JUN 과 JNK 의 인산화에 의해 전립선암 세포주의 세포 사멸을 유도하였다. 생체 내 연구에서 CKD-516 과 PD-1 항체를 모두 사용하였을 때 상당한 시너지 효과가 나타났으며, 종양 성장

억제 비율은 병용 요법 그룹에서 유의하게 높았다. (CKD-516 3mg / kg 에서 34.64 %, CKD-516 3mg/kg 및 항 PD-1 병용 요법에서 90.69 %). 수지상세포의 성숙은 CKD-516 에 의해 유도되었으며 CD80 및 CD86 과 같은 세포 표면 마커의 발현이 크게 증가하였다.

결론: CKD-516 은 종양 세포의 전립선암 세포의 사멸을 유도하는 유망한 치료제이며 면역 관문 억제제와 병용하였을 때 항암 효과를 향상시킨다.

중심단어; 전립선암 세포주, CKD-516, 혈관 저해제, PD-1 항체